Expression of STAT3 in Prostate Cancer Metastases

Don-Doncow, Nicholas; Marginean, Felicia; Coleman, Ilsa; Nelson, Peter S.; Ehrnström, Roy; Krzyzanowska, Agnieszka; Morrissey, Colm; Hellsten, Rebecka; Bjartell, Anders

Published in:
European Urology

DOI:
10.1016/j.eururo.2016.06.018

2017

Document Version:
Peer reviewed version (aka post-print)

Expression of STAT3 in prostate cancer metastases

Nicholas Don-Doncow[1], Felicia Marginean[1,2], Ilsa Coleman[3], Peter S Nelson[3], Roy Ehrnström[2], Agnieszka Krzyzanowska[1], Colm Morrissey[4], Rebecka Hellsten[1], Anders Bjartell[1,5].

1 Department of Translational Medicine, Division of Urological Cancers, Malmö, Lund University, Sweden,
2 University and Regional Laboratories Region Skåne, Department of Pathology, Skåne University Hospital Malmö, Sweden
3 Fred Hutchinson Cancer Research Center, Seattle, Washington, USA
4 Department of Urology, University of Washington, Seattle, Washington, USA
5 Department of Urology, Skåne University Hospital, Malmö, Lund University, Sweden

Corresponding Author: Anders Bjartell, Department of Urology, Skåne University Hospital, Jan Waldenströms Gata 5, SE-205 02, Malmö, Sweden, Tel: +4640336398, Fax: +4640336911, email: anders.bjartell@med.lu.se

Key words: castration-resistant, metastases, prostate cancer, STAT3, tissue microarray

Author Contributions:
Study concept and design: Bjartell, Hellsten, Morrissey
Acquisition of data: Don-Doncow, Marginean, Coleman, Morrissey, Bjartell
Analysis and interpretation of data: Don-Doncow, Marginean, Coleman, Nelson, Ehrnström, Krzyzanowska, Morrissey, Hellsten, Bjartell
Drafting of the manuscript: Don-Doncow, Hellsten, Bjartell
Critical revision of the manuscript for important intellectual content: Krzyzanowska, Morrissey, Hellsten, Bjartell
Statistical analysis: Don-Doncow, Coleman, Nelson
Obtaining funding: Bjartell

Acknowledgements: The authors wish to thank Elise Nilson and Kristina Ekström-Holka for carrying out the immunohistochemical staining and Giacomo Canesin for the western blot analysis.
We thank the patients and their families who were willing to participate in the Prostate Cancer Donor Program. The investigators Drs. Robert Vessella, Celestia Higano, Bruce Montgomery, Evan Yu, Paul Lange, Martine Roudier, and Lawrence True for their contributions to the University of Washington Medical Center Prostate Cancer Donor Rapid Autopsy Program. This research was supported by funding by the Pacific Northwest Prostate Cancer SPORE (P50CA97186), the PO1 NIH grant (PO1CA085859), R01 CA165573, the Richard M. LUCAS Foundation, the Swedish Cancer Foundation, the Swedish Research Council, Lund University (ALF), the Malmö University Hospital Research Foundations and the Gunnar Nilsson's Cancer Foundation.

Article word count without abstract: 1001
Abstract word count: 179

Abstract

STAT3, and its upstream activator IL6R, have been implicated in the progression of prostate cancer and are possible future therapeutic targets. We analyzed 223 metastatic samples from rapid autopsies of 71 patients who had died of castration-resistant prostate cancer (CRPC) in order to study protein and gene expression of pSTAT3 and IL6R. Immunohistochemical analysis revealed that 95% of metastases were positive for pSTAT3 and IL6R with varying expression levels. Bone metastases showed significantly higher expression of both pSTAT3 and IL6R compared with lymph node and visceral metastases. STAT3 mRNA levels were significantly higher in bone compared to lymph node and visceral metastases, whereas no significant difference in IL6R mRNA expression was observed.

Our study strongly supports the suggested view of targeting STAT3 as a therapeutic option in patients with mCRPC.

Patient Summary:

We studied the levels of two proteins (pSTAT3 and IL6R) in metastases from patients who died from castration-resistant prostate cancer. We found high levels of pSTAT3 and IL6R in the bone metastasis, suggesting that these proteins may be targets for new anti-cancer drugs.

Treatment of locally advanced and metastatic prostate cancer (PCa) is currently hampered by drug resistance, with an urgent need to identify new therapeutic targets. A recently explored candidate target for the treatment of aggressive PCa is the transcription factor Signal Transducer and Activator of Transcription 3 (STAT3)[1,2]. STAT3 is an important oncogenic-associated protein found to be constitutively activated in PCa[3,4]. After activation via phosphorylation, STAT3 translocates to the nucleus and acts on the transcription of several genes involved in anti-apoptosis, proliferation and metastasis (e.g. BCL-2, MCL1, Cyclin D1 and MMP9)[1]. Phosphorylation of the 705 tyrosine residue in the STAT3 protein is correlated with aggressive PCa and high Gleason score[4]. Interleukin-6 (IL6) has been shown to be a main driving force in pSTAT3 activation, and was found to be highly expressed in PCa patients with a worse prognostic outcome[5]. The cell surface interleukin-6 receptor (IL6R) has also been implicated in cancer progression[3]. As the expression of pSTAT3 in PCa metastases is not fully clarified, we immunostained a unique cohort consisting of 223 tumor samples obtained from 71 CRPC patients from the Prostate Cancer Donor Rapid Autopsy Program at the University of Washington (Seattle, WA)[6], for both pSTAT3 and its upstream activator IL6R. All patients were on androgen-deprivation therapy (ADT) and most had been treated with chemotherapy. Patient samples were available from bone, lymph node and visceral metastases (Supplementary Tables 1 and 2). Immunostaining for pSTAT3 was nuclear, and was evaluated by the use of a scoring index, recording both the intensity (0, 1, 2, and 3, Fig. 1A-D) and the percentage of tumor cells stained: 1 (0-10%), 2 (11-75%) and 3 (above 75%). These scores were then multiplied to create an expression score, which ranged from 0-9. Immunostaining for IL6R was cytoplasmic, membranous and ubiquitous leading to scoring based solely on intensity: 0, 1, 2, and 3 (Fig. 1E-H).

We found that 99% of bone, 96% of lymph node and 86% of visceral metastases expressed pSTAT3 (Fig. 1I). The average pSTAT3 expression score was the highest in bone (5.23±2.40), followed by lymph node (3.78±2.42) and visceral (2.59±2.11) metastases. Matched samples of all three tissue types were available for 24 patients, where we found similar results to those observed in the entire group of tumors, with significant differences in pSTAT3 expression observed between the bone and lymph node and visceral metastases (Fig. 1J).

IL6R was expressed in 99% of bone, 88% of lymph node and 92% of visceral metastases (Fig. 1 K). The average IL6R expression score was significantly higher in bone (2.20±0.66) than lymph node (1.68±0.94) but not compared to visceral (1.96±0.88) metastases. For 23 patients with matched tumors, bone expression was higher than in non-matched patients, leading to significantly higher IL6R expression in the bone tissue compared with both the lymph node and visceral metastases (Fig. 1L).

Co-expression of pSTAT3 and IL6R was observed in 98% of bone, 84% of lymph node and 78% of visceral metastases (data not shown).

A subset of 63 patients with 149 unique tumor samples was available for transcript abundance analysis of STAT3 and IL6R mRNA expression. STAT3 mRNA levels were significantly highest in bone, mirroring the IHC results for pSTAT3. There was no significant difference in IL6R mRNA expression between the different metastatic sites (Fig. 2).

Recently published data indicates that the location of metastasis plays a role in the overall survival in patients with metastatic disease[7]. In our study, we observed that the levels of pSTAT3 were significantly higher in bone compared to lymph node and visceral metastases suggesting that tissue location may dictate pSTAT3 expression

levels. When looking specifically at patients with all three tissue sites of metastases available, it was apparent that pSTAT3 expression levels were heterogeneous within each patient, with highest expression in the bone, similar to earlier published results on downstream targets of STAT3 in a similar cohort[8].

Bone metastases can be either osteolytic or osteoblastic with the majority of bone lesions in PCa being the latter. Osteoblasts are known to express IL6, supporting the theory of a tissue-specific microenvironment that stimulates the activation of pSTAT3[9]. Moreover a recent publication has shown that IL6 expression in bone is derived from endothelial cells in the blood vessels and not the tumor cells themselves[10]. However, further investigation is needed to better understand why pSTAT3 is highly expressed in bone metastases in CRPC patients. It is unlikely that our findings are related to an artifact caused by the decalcification process, as this process did not affect the immunostaining intensity in soft tissue (Supplementary Fig. 1). Our antibodies have been validated, details available in supplementary materials.

It is interesting to note that in our cohort, over 95% of patients expressed some level of pSTAT3, suggesting that phosphorylation of STAT3 is a common event in metastatic CRPC, which is in line with current hypotheses that STAT3 activation is commonly found in aggressive PCa cells. Further, we observed higher STAT3 mRNA levels in the bone tissue compared to lymph and visceral tissue mirroring our results of pSTAT3 immunostaining. Correlation analysis did not reveal strong associations between either pSTAT3 and IL6R at the IHC level or STAT3 and IL6R at the mRNA level, but co-expression of pSTAT3 and IL6R in IHC was seen in a high number of samples (Supplementary Table 3), indicating that expression levels of pSTAT3 may be influenced by other signaling pathways in addition to IL6R, such as EGF or other cytokines[1]. These results need to be further evaluated in larger cohorts.

Our data suggests pSTAT3 is a potential therapeutic target in metastatic CRPC. Bone metastases presented the highest expression of both pSTAT3 in IHC and STAT3 mRNA, suggesting an environmental niche created by the bone tissue that favors high pSTAT3 expression. Follow-up studies are needed to better understand what regulates expression of pSTAT3 in metastases from different organs. Notwithstanding, due to its widespread presence in metastatic CRPC, directly targeting STAT3 presents a viable future treatment of patients in late stage prostate cancer.

References

1. Bishop JL, Thaper D, Zoubeidi A. The Multifaceted Roles of STAT3 Signaling in the Progression of Prostate Cancer. *Cancers.* 2014;6(2):829-859.

2. Canesin G, Evans-Axelsson S, Hellsten R, et al. The STAT3 Inhibitor Galiellalactone Effectively Reduces Tumor Growth and Metastatic Spread in an Orthotopic Xenograft Mouse Model of Prostate Cancer. *European urology.*

3. Tam L, McGlynn LM, Traynor P, Mukherjee R, Bartlett JM, Edwards J. Expression levels of the JAK/STAT pathway in the transition from hormone-sensitive to hormone-refractory prostate cancer. *Br J Cancer.* Aug 6 2007;97(3):378-383.

4. Mora LB, Buettner R, Seigne J, et al. Constitutive activation of Stat3 in human prostate tumors and cell lines: direct inhibition of Stat3 signaling induces apoptosis of prostate cancer cells. *Cancer Res.* Nov 15 2002;62(22):6659-6666.

5. Shariat SF, Andrews B, Kattan MW, Kim J, Wheeler TM, Slawin KM. Plasma levels of interleukin-6 and its soluble receptor are associated with prostate cancer progression and metastasis. *Urology.* 12// 2001;58(6):1008-1015.

6. Roudier MP, True LD, Higano CS, et al. Phenotypic heterogeneity of end-stage prostate carcinoma metastatic to bone. *Human Pathology.* 7// 2003;34(7):646-653.

7. Halabi S, Kelly WK, Ma H, et al. Meta-Analysis Evaluating the Impact of Site of Metastasis on Overall Survival in Men With Castration-Resistant Prostate Cancer. *Journal of Clinical Oncology.* March 7, 2016 2016.

8. Akfirat C, Zhang X, Ventura A, et al. Tumor Cell Survival Mechanisms in Lethal Metastatic Prostate Cancer Differ Between Bone and Soft Tissue Metastases. *The Journal of pathology.* 2013;230(3):291-297.

9. Lu Y, Zhang J, Dai J, et al. Osteoblasts induce prostate cancer proliferation and PSA expression through interleukin-6-mediated activation of the androgen receptor. *Clinical & Experimental Metastasis.* 2004;21(5):399-408.

10. Yu S-H, Zheng Q, Esopi D, et al. A Paracrine Role for IL6 in Prostate Cancer Patients: Lack of Production by Primary or Metastatic Tumor Cells. *Cancer Immunology Research.* October 1, 2015 2015;3(10):1175-1184.

Legends to Illustrations

Figure 1: Examples of IHC staining and distribution of IHC expression scores for pSTAT3 and IL6R

A-D: Examples of pSTAT3 staining in metastases. **A:** Negative (0) liver staining **B:** Low (1) lymph node staining. **C:** Medium (2) lymph node staining. **D:** High (3) bone staining. **E-H:** Examples of IL6R staining in metastases. **E:** Negative (0) liver staining. **F:** Low (1) lymph node staining **G:** Medium (2) lymph node staining. **H:** High (3) bone staining. Scale bar=100µM.

I-L: Expression in bone vs. lymph node vs. visceral metastases. **I:** Overall tissue sample distribution for pSTAT3 staining, significant differences observed between bone (n=113), lymph node (n=51) and visceral (n=51) metastases. **J:** Matched tissue samples for pSTAT3 staining (n=24), significant differences observed between bone and both lymph node and visceral metastases. **K:** Overall tissue samples for IL6R staining, significant differences only observed between bone (n=117) and lymph node (n=50) metastases, no significant differences were observed between bone and visceral metastases (n=50) **L:** Matched tissue samples for IL6R staining (n=23), significant differences observed between bone and both lymph node and visceral metastases. **I and J:** scoring index: "zero"=0; "low"=1&2, "medium"=3&4, "high"=6&9. **K and L:** scoring index: "zero"=0; "low"=1, "medium"=2, "high"=3. Asterisks denote significant differences between groups by Wilcoxon signed-rank test (* $p \leq 0.05$, ** $p \leq 0.01$, *** $p \leq 0.001$).

Figure 2: mRNA levels in bone vs. lymph node vs. visceral metastases.

mRNA expression scores (log2 signal intensity of Cy3) for bone, lymph node and visceral metastases. Asterisks denote significant differences between groups by Wilcoxon signed-rank differences (*** $p \leq 0.001$). Significant differences were observed between bone STAT3 and both lymph node and visceral STAT3 mRNA levels. No significant differences were observed in IL6R expression between the different sites of metastasis.

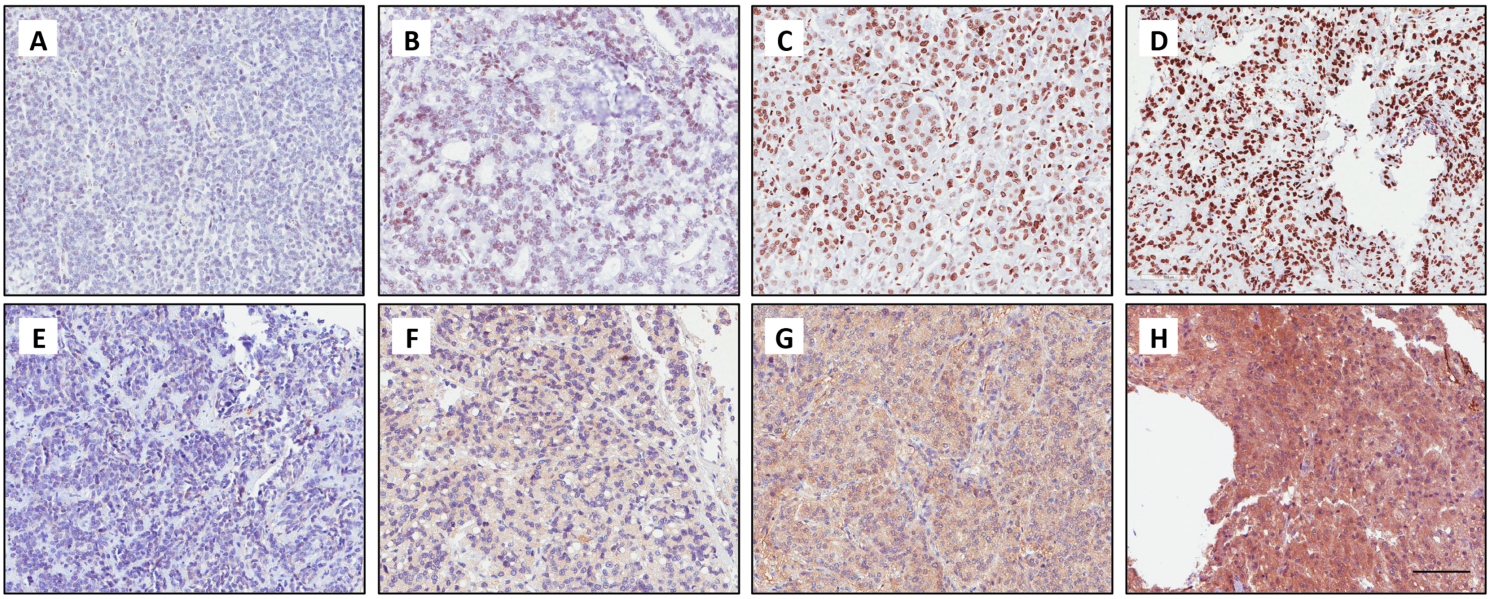
A
B
C
D
E
F
G
H

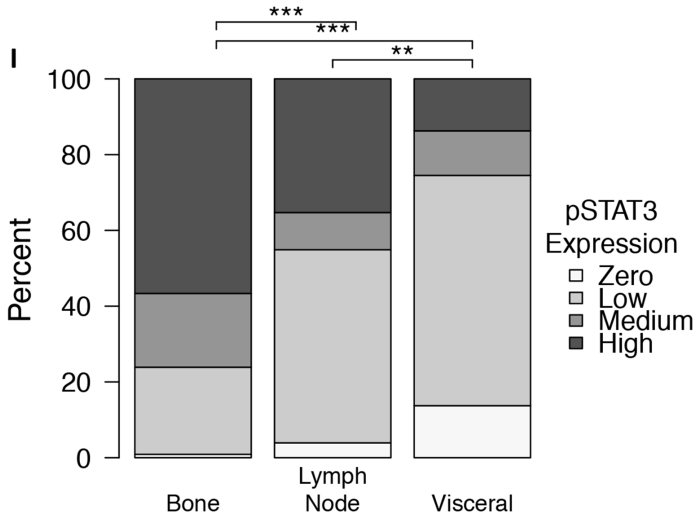
I
***
***
**
100
80
60
40
20
0
Percent
Bone
Lymph Node
Visceral
pSTAT3 Expression
Zero
Low
Medium
High

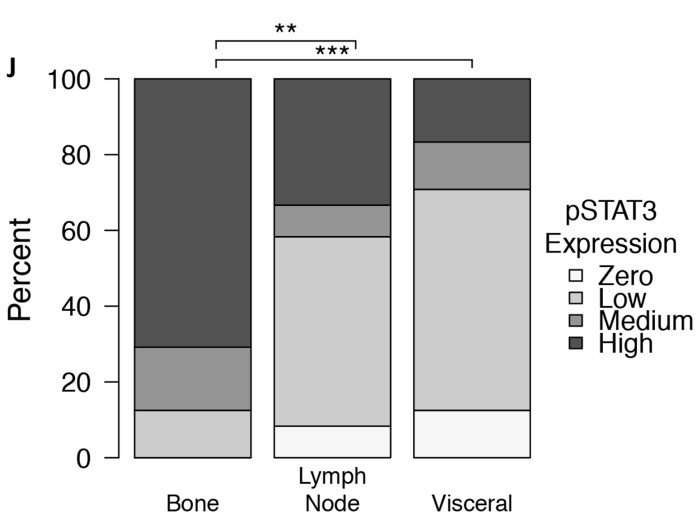
J
**
***
100
80
60
40
20
0
Percent
Bone
Lymph Node
Visceral
pSTAT3 Expression
Zero
Low
Medium
High

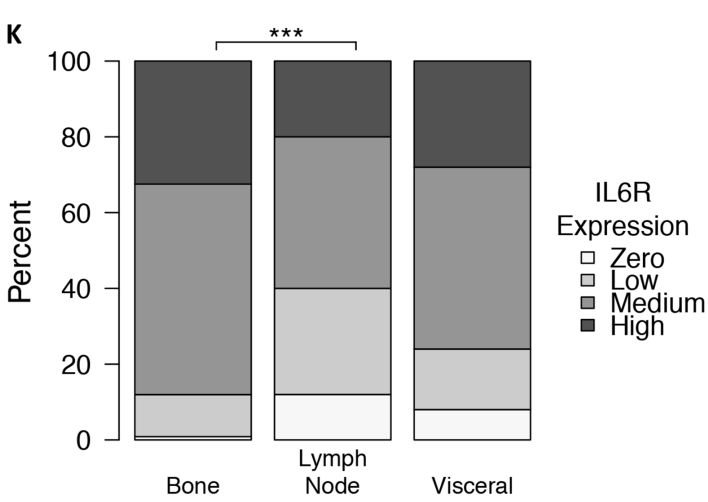
K
***
100
80
60
40
20
0
Percent
Bone
Lymph Node
Visceral
IL6R Expression
Zero
Low
Medium
High

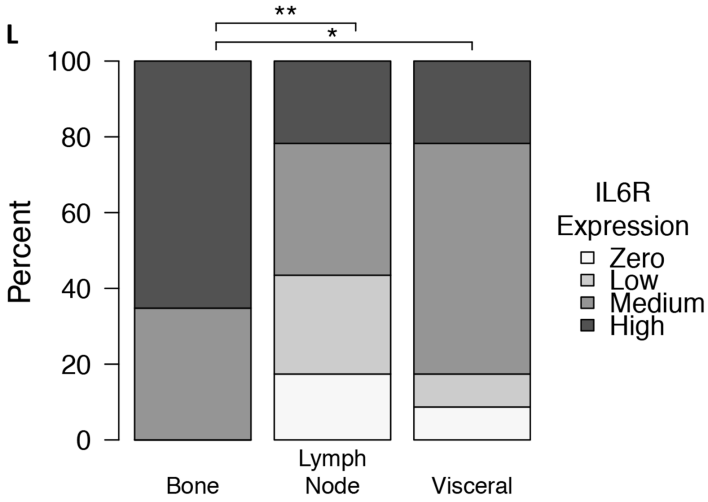
L
**
*
100
80
60
40
20
0
Percent
Bone
Lymph Node
Visceral
IL6R Expression
Zero
Low
Medium
High

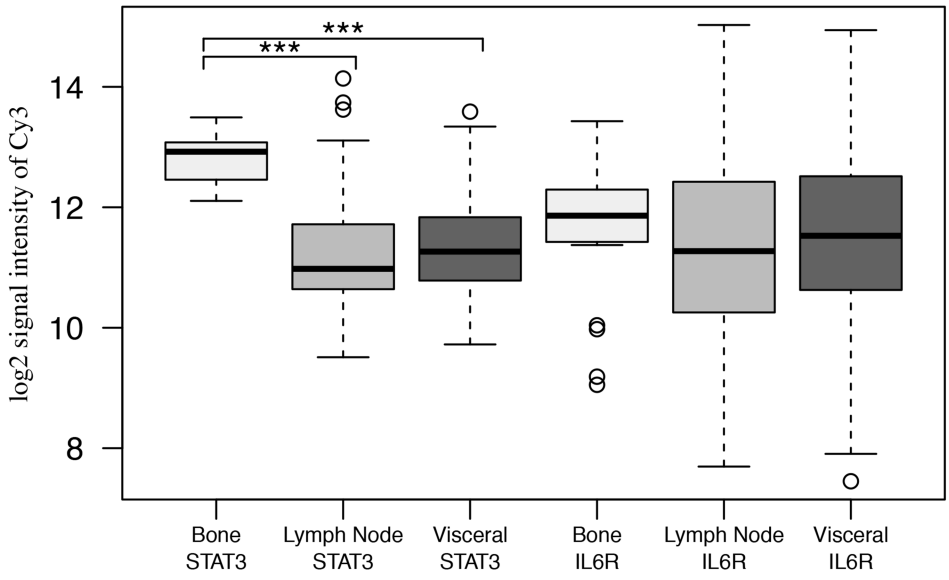
***
***
14
12
10
8
log2 signal intensity of Cy3
Bone
STAT3
Lymph Node
STAT3
Visceral
STAT3
Bone
IL6R
Lymph Node
IL6R
Visceral
IL6R

Supplementary material

Patient material

Samples were obtained from patients who died of metastatic castration-resistant prostate cancer (CRPC) and who signed written informed consent for a rapid autopsy performed within 6 h of death, under the aegis of the Prostate Cancer Donor Program at the University of Washington [1]. The Institutional Review Board of the University of Washington approved this study. Patient characteristics are detailed in Supplementary Table 1. All of the samples were obtained from autopsy performed 2–6 h after death from CRPC. All patients were on androgen deprivation therapy and most were being treated with chemotherapy. Multiple metastatic samples were collected from 71 CRPC patients: the 223 unique samples comprised 119 from bone, 52 from lymph node, and 52 from visceral metastases (Supplementary Table 2). Of these 71 patients, 24 had matched tissue samples available with at least one sample of bone, lymph node, and visceral metastases for pSTAT3 staining, but owing to loss of a few cores for IL6R stained slides, only 23 matched samples were available. For a subset of this cohort (n = 63), we had access to 149 samples from 20 bone, 68 lymph node, and 61 visceral metastases for mRNA analyses.

Immunohistochemistry (IHC)

Tissues were available in a tissue microarray (TMA) format. Deparaffinized 5μm sections from the TMA blocks were subjected to antigen retrieval using a PT-Link module (Dako, Glostrup, Denmark) at 95–99°C for 20 min in citric acid buffer (0.01 M, pH 6.0). Then immunostaining for pSTAT3 (9131, 1:50 dilution; Cell Signaling, Danvers, USA) and IL6R (ab128008, 1:600 dilution; Abcam, Cambridge, UK) was performed using EnVision Flex high-pH reagent (Dako) in an Autostainer Plus system according to the manufacturer's protocol.

Bone samples were decalcified in 10% formic acid before paraffin embedding. To investigate whether this decalcification process had any influence on immunostaining efficacy, a piece of soft tissue (breast) was subjected to decalcification treatment before routine processing. Immunostaining was then compared between normally processed and decalcified tissue for pSTAT3 and IL6R antibodies. No difference in immunostaining intensity or pattern was observed (Supplementary Fig. 1).The pSTAT3 antibody was validated by western blotting of cell lysates from three cell lines; DU145, long-term IL6-stimulated LNCaP (both positive for pSTAT3), and LNCaP (negative for pSTAT3; Supplementary Fig. 2). The IL6R antibody has previously been used for IHC. The IL6R IHC staining intensity was correlated with *IL6R* mRNA expression, indicating specificity of the IL6R antibody [2].

Immunostaining scoring

Immunostained sections were scored independently by two of the authors (ND and FM; the latter is a fully certified pathologist); in the case of initial disagreement, consensus was reached after open discussion. As expected, immunostaining was nuclear for pSTAT3 and cytoplasmic and membranous for IL6R. Owing to the ubiquitous staining of IL6R, scoring was based only on intensity and split into four categories: 0 (negative), 1 (low), 2 (medium), and 3 (high). For interpretation of pSTAT3 immunostaining, we used a scoring index that recorded both the intensity (0, 1, 2, and 3 as above) and the percentage of tumor cells stained, subdivided into three categories: 1, 0–10%; 2, 11–75%; and 3, >75%. These scores were then multiplied to create an expression score, which ranged from 0 to 9.

Microarray analysis

A total of 149 tumors from 63 patients were profiled via expression microarray. A Leica CM3050S cryostat was used to cut 8-μm sections, which were collected on PEN membrane frame slides (Life Technologies) and immediately fixed in 95% ethanol. Sections were briefly stained (5–10 s) with Mayer's hematoxylin solution (Sigma-Aldrich) and then dehydrated in 100% ethanol. Laser capture microdissection was performed with an Arcturus Veritas instrument using both UV cutting and infrared capture lasers with CapSure Macro LCM Caps (Life Technologies), and 5000–10 000 tumor cells were collected per sample. Digital photographs were taken of tissue sections before, during, and after LCM and assessed by a pathologist to confirm the tumor content. Following LCM, captured cells were lysed in Arcturus RNA extraction buffer. RNA was isolated using an Arcturus PicoPure RNA isolation kit and was treated with DNAse using a Qiagen RNase-free DNase set. Bone metastases were sampled using a 1-mm-diameter tissue punch for frozen OCT-embedded tumors in a –20°C cryostat. Samples were obtained from the region of the block where there was tumor on the basis of a section of an adjacent decalcified FFPE block. RNA was isolated from the tissue cores using a Qiagen RNeasy Plus Micro kit. Total RNA from all tumors was then amplified for two rounds using an Ambion Message Ampa RNA kit. Probe labeling and hybridization to Agilent 44K whole human genome expression oligonucleotide microarray slides (Agilent Technologies, Santa Clara, CA, USA) was performed according to the manufacturer's recommendations, and fluorescent array images were collected using an Agilent G2565BA DNA microarray scanner. Agilent feature extraction software was used to grid and extract the data. Data were loess normalized within arrays (normexp background correction with offset 50) and quantile normalized between arrays in R using the Limma Bioconductor package by batch. Control probes were removed, duplicate probes were averaged, and spots flagged by the feature extraction software as being foreground feature nonuniformity or population outliers were assigned a value of NA. An additional normalization step was applied to remove systematic batch effects due to the date of RNA amplification by applying the ComBat function within the svaBioconductor package to the log2 Cy3 signal intensities.

Statistical methods

All statistical tests were carried out in R using R studio (www.rstudio.com). Correlations were tested using the Pearson correlation coefficient, while between-group comparisons were performed using a Wilcoxon signed-rank test. For mRNA expression, the log2 Cy3 adjusted intensities were used for analysis. Statistical significance was set to $p < 0.05$.

Supplementary Fig. 1 – Normal versus decalcified tissue. Breast tissue was obtained and split into two parts; one was subjected to decalcification and then processed as normal, while the other was processed normally. Staining results are shown for (A,C) pSTAT3 and IL6R staining, respectively, of normally processed tissue, and (B,D) decalcified tissue. The staining intensity did not differ. Scale bar, 100 μm.

Supplementary Fig. 2 – Validation of the pSTAT3 antibody. Western blot showing the specificity of the pSTAT3 antibody. pSTAT3 was detected in DU145 cells but not in unstimulated LNCaP cells. LNCaP cells subjected to long-term IL6 stimulation showed upregulation of pSTAT3.

Supplementary Table 1 – Patient characteristics

Parameter	Patients, *n* (%)
Age at time of diagnosis	
Mean, yr (median)	63.7 (63.3)
<50 yr	3 (4.2)
50–59 yr	24 (33.8)
60–69 yr	25 (35.2)
>70 yr	18 (25.4)
Unknown	1 (1.4)
Age at time of death	
Mean, yr (median)	71 (71.3)
<50 yr	2 (2.8)
50–59 yr	7 (9.9)
60–69 yr	23 (32.4)
>70 yr	39 (54.9)
Unknown	0
Survival time from diagnosis to death	
Mean, yr (median)	7 (5.8)
<7 yr	40 (56.3)
>7 yr	30 (42.3)
Unknown	1 (1.4)
Gleason score for primary tumor	
≤6	4 (5.6)
7	19 (26.8)
8	6 (8.5)
≥9	26 (36.6)
Unknown	16 (22.5)

Supplementary Table 2 – Tissue sample types and frequencies

Tissue	Samples, *n* (%)
Bone	119 (53.4)
Lymph node	52 (23.3)
Liver	27 (12.1)
Lung	14 (6.3)
Spleen	2 (0.9)
Appendix	1 (0.45)
Kidney	3 (1.4)
Pleura	1 (0.45)
Adrenal gland	2 (0.9)
Diaphragm	2 (0.9)

Supplementary Table 3 – Correlation between IL6R and pSTAT3, and IL6R and STAT3 expression

Tissue	*r*
pSTAT3 and IL6R protein expression	
Bone	0.16 NS
Lymph node	0.06 NS
Visceral	–0.01 NS
STAT3 and *IL6R* mRNA expression	
Bone	0.26 NS
Lymph node	0.263 *
Visceral	0.416 ***

r = correlation coefficient; NS = not significant.

References

1. Roudier MP, True LD, Higano CS, et al. Phenotypic heterogeneity of end-stage prostate carcinoma metastatic to bone. Hum Pathol 2003;34:646–53.
2. Sindhu S, Thomas R, Shihab P, Sriraman D, Behbehani K, Ahmad R. Obesity is a positive modulator of IL-6R and IL-6 expression in the subcutaneous adipose tissue: significance for metabolic inflammation. PLoS One 2015;10:e0133494.

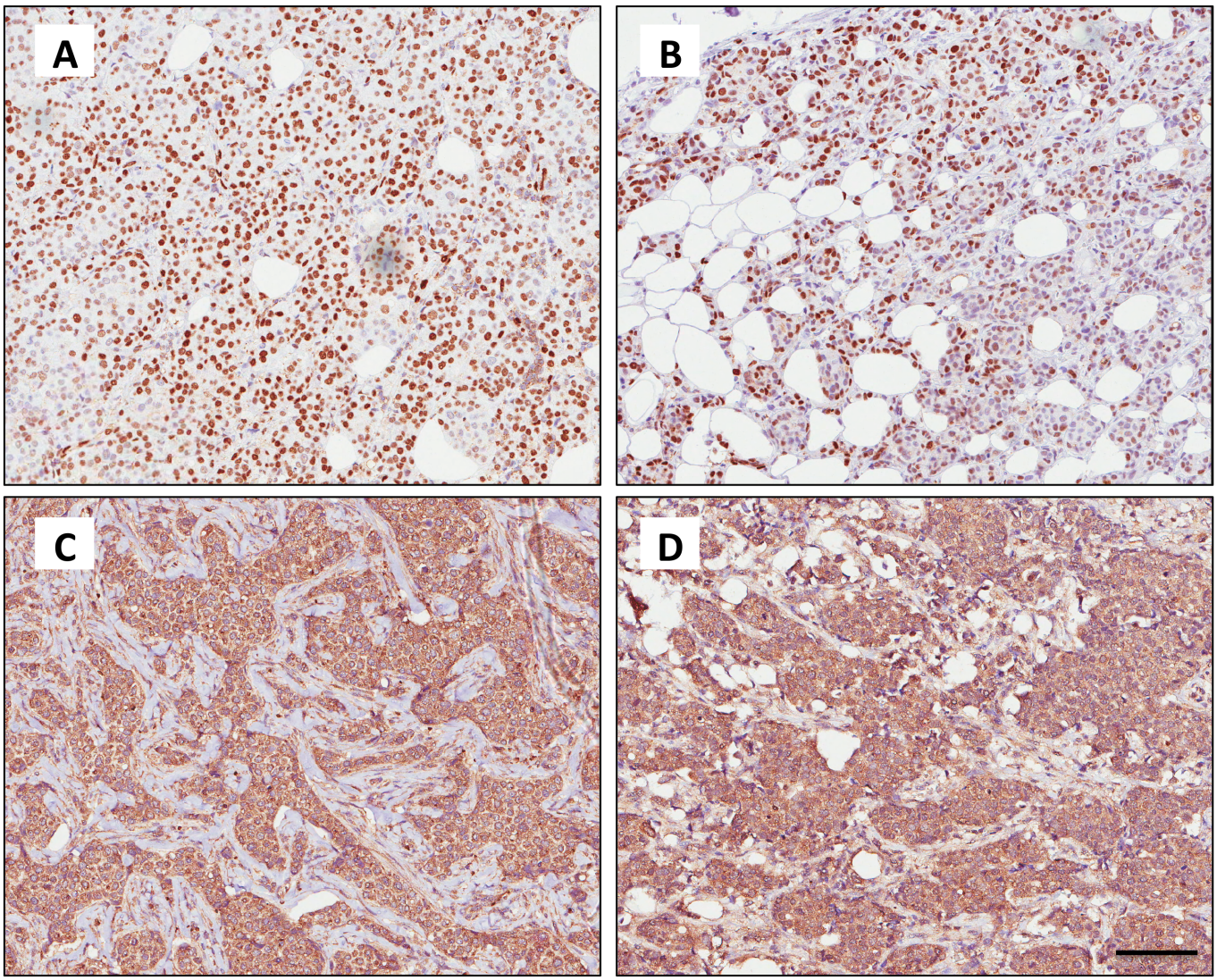

Supplementary Figure 1: Normal vs. decalcified tissue
Breast tissue was obtained and split into two parts; one underwent decalcification and was then processed as normal while the other was normally processed. The results of the staining are seen here with **A** and **C** representing normal staining of pSTAT3 and IL6R respectively and **B** and **D** representing decalcified tissue stained for pSTAT3 and IL6R respectively. Staining intensity was unchanged. Scale bar=100µM.

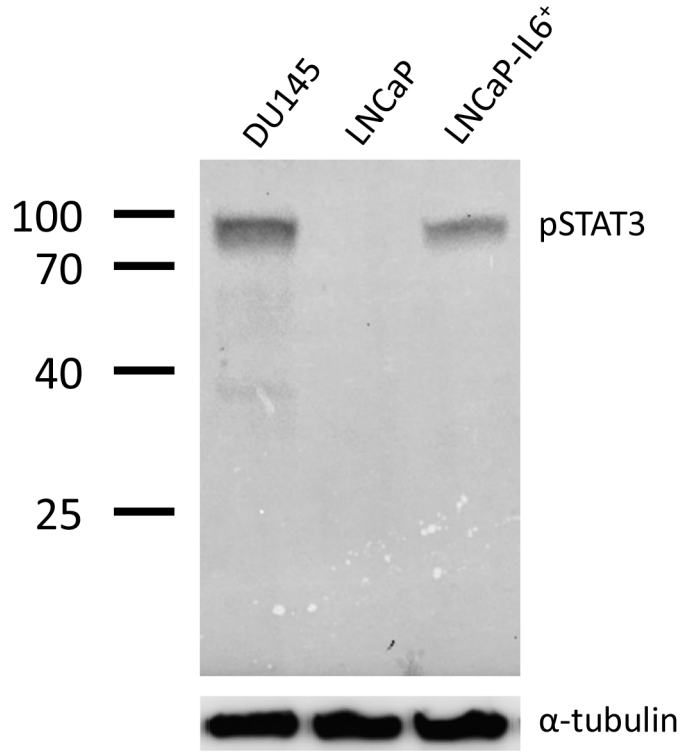
DU145
LNCaP
LNCaP-IL6+
100
70
40
25
pSTAT3
α-tubulin